A Position and Orientation Compensation Mechanism for Automatic Docking Device of Launch Rocket

Zhou Cheng *, *Yu Cungui*

School of Mechanical Engineering, Nanjing University of Science and Technology, Nanjing 210094, P. R. China

(Received 28 June 2017; revised 2 October 2018; accepted 5 December 2018)

Abstract: A position and orientation compensation mechanism for the automatic docking device of a launch rocket was established. The docking process was simulated, and the maximum docking deviation was used for the prototype testing of the compensation mechanism. The compensation mechanism mainly comprises four column pairmotion branch chains with the same structure. When the position of the ground connector panel changes relative to the moving platform, the sliding rods in the four motion branch chains move and rotate to either compress or stretch the connected spring, thereby compensating the position and orientation. First, the dynamic simulation model of the compensation mechanism was established. The docking process was then simulated under the maximum docking deviation. Bench testing of the automatic docking device prototype was carried out. Afterwards, the device was manufactured, and a maximum load test and maximum deviation test were carried out. The results demonstrate that the compensation mechanism meets the design requirements, and the spring stiffness was found as the most important factor in determining the mechanical properties of the system. The proposed compensation mechanism has a number of advantages, including a simple structure, large load bearing capacity, small size, simple installation, and adjustment.

Key words: priming connector; position and orientation compensation mechanism; spring; dynamic simulation; prototype test

CLC number: V19 **Document code**: A **Article ID**: 1005-1120(2018)06-1064-09

0 Introduction

To shorten propellant filling time, improve emission efficiency, and eliminate the personal safety risks associated with manual docking of launch rockets, automatic docking technology has gained a great deal of attention in many countries[1-3]. In the early 1960s, the integrated connector panel used by the early Saturn V carrier rocket in the United States already offered a certain degree of automatic docking capabilities[4-5]. Further studies in the United States, Russia, France, and other countries resulted in the development of "Arrow" docking technology and "Shelter" docking technology led by the United States and Russia, respectively[6-7]. The "Arrow" docking technology avoids problems associated with alignment and additional problems caused by shaking of the arrow body during the docking and filling process. However, repeated docking cannot be achieved. The "Shelter" docking technology provides a simple and reliable process for docking and disengagement with short operation time and a reconnecting function after docking. However, it is classified as rigid assembly technology, therefore, its adaptability to the environment is poor and the filling port can only be located at the tail end of the arrow. While each docking technology has certain advantages and disadvantages, the technologies have yet to be fully integrated together.

Other docking technologies, including the "amphibious integrated" and "flexible shelf" docking technologies, are based on "Arrow" and

* Corresponding author, E-mail address: zhoucheng@njust.edu.cn.

How to cite this article: Zhou Cheng, Yu Cungui. A position and orientation compensation mechanism for automatic docking device of launch rocket[J]. Trans. Nanjing Univ. Aero. Astro., 2018, 35(6): 1064-1072.
http://dx.doi.org/10.16356/j.1005-1120.2018.06.1064

"Shelter". The "amphibious integrated" system is currently under development in China. The amphibious robot system prototype developed in our laboratory can be divided into a number of different docking stages, corresponding to the different docking modes[8-11]. The "flexible shelf" docking technology is based solely on the "Shelter" technology, replacing the rigid assembly with a more flexible assembly[12]. The docking technology therefore has the advantages of "Shelter", and in addition avoids any damage that may be caused by the huge tear forces of the rigid bottom joint. Furthermore, restrictions on the filling port location associated with the rigid "Shelter" technology have yet to overcome.

In this study, the position and orientation compensation mechanism is classified as "flexible shelf" docking technology. The flexible connection is achieved by the compensation mechanism. It compensates the position and orientation difference produced from the docking motion by passive deformation. It converts the rigid connection between the docking device and arrow body into a flexible connection, reducing damage to the arrows by providing a protective effect and is also beneficial to successful docking. Thus, aposition and orientation compensation mechanism is presented in this study based on specific design requirements. In addition, the proposed mechanism was simulated and experimentally validated.

1 Design of Position and Orientation Compensation Mechanism

1.1 Docking device of launch rocket

The structure of the automatic docking device is shown in Fig. 1, and the device consists of the actuating mechanism (3-PSS parallel mechanism)[13-16], moving platform, position and orientation compensation mechanism, ground connector panel, rocket connector panel, centering guide structure, and retaining mechanism. The rocket connector panel in Fig. 1 is a part of the launch rocket, which is not shown. The compensation mechanism is installed between the moving platform and ground connector panel, and the moving platform is fixed at the end of the actuating mechanism. While docked, the rocket is filled with propellant and the actuating mechanism drives the moving platform, thereby driving the ground connector panel close to the rocket connector panel. After the completion of the docking process, the ground connector panel and rocket connector panel are locked with the retaining mechanism. During the propellant filling process, the rocket can be affected by loads due to wind and can randomly shake, causing the rocket connector panel to move in six directions[17]. When this occurs, the compensation mechanism can compensate for the offset between the panel of the rocket connector and the moving platform, and thus protects the rocket.

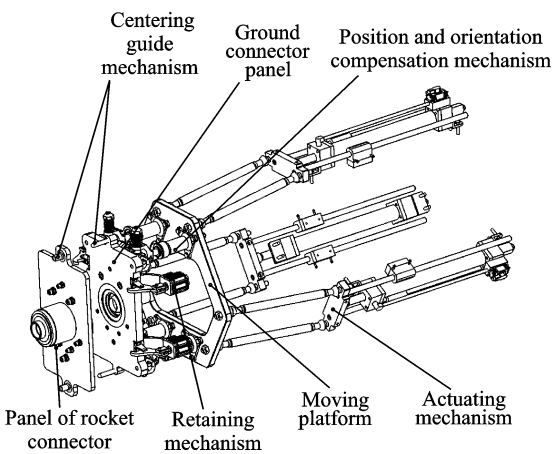

Fig. 1 Structural diagram of docking device

1.2 Design requirements for position and orientation compensation mechanism

Based on the docking conditions, the position and orientation compensation mechanism must meet the following requirements:

(1) To achieve a flexible connection between the automatic docking device and rocket, the compensation mechanism must have six degrees of freedom. According to the error analysis, the compensation mechanism has a maximum compensation value of ± 8 mm in three translational directions, and a maximum angle compensation of $\pm 0.5°$ in three rotational directions.

(2) The position and orientation compensa-

tion mechanism must have a certain amount of load bearing capacity. Before docking, the combined mass of the ground connector panel, retaining mechanism, and pipeline is approximately 35 kg, and the fuel in the pipeline is approximately 15 kg. Therefore, the compensation mechanism must be able to support a total mass of approximately 50 kg.

(3) The maximum contact force between the ground connector panel and rocket connector panel must be no greater than 3 000 N during the docking and servomechanism process.

In addition to the above factors, the design of the compensation mechanism should meet a number of other conditions such assimple structure, large load bearing capacity, small size occupying minimal space, simple installation and adjustment as much as possible.

1.3 Structural design of position and orientation compensation mechanism

The position and orientation compensation mechanism encompasses elements of three types of mechanisms: compliant, series, and parallel. A compliant mechanism transmits motion and energy via the elastic deformation of some or all of its flexible components[18]. Therefore, compliant mechanism encounters difficulties in withstanding the total quality of the ground connector panel and meeting the size requirements for the compensation space. The series design has a simple structure, large range of motion, low cost, and more mature technology. However, using a series mechanism with six degrees of freedom to realize compensation in all the directions requires more space and the structure will be overstaffed. Compared with the series mechanism, the parallel mechanism has the advantages of a large load bearing capacity, high structural stiffness, superior precision motion control, and compactness[16-19]. The parallel mechanism has important applications in motion simulators, industrial robots, parallel machine tools, medical robots, and micro robots[18]. The position and orientation compensation mechanism design presented in this study is based on parallel mechanism and has the following advantages: (1) This instrument based on the technology has high rigidity and strength, resulting in a higher load bearing capacity; (2) The size of the front and rear space is small, and the structure is compact; (3) The overall mass is significantly reduced compared to that in the series mechanism.

The structure of the proposed position and orientation compensation mechanism is shown in Fig. 2, and it mainly consists of four CCC (C refers to the column pair) motion branch chains with identical structures. Each motion branch chain includes a front and rear sliding rod, sleeve, end cap, front and rear springs, C-type component, up and down sliding rods, up and down springs, up and down adjusting nuts, left and right sliding rods, left and right spring, and left and right adjusting nuts. All the connections between the front and rear sliding rods and sleeve, up and down sliding rods and front and rear sliding rods, and left and right sliding rods and up and down sliding rods are column pairs. In each motion branch chain, the spring is set on the sliding rod. When the position of the ground connector panel changes relative to the moving platform, the sliding rods in the four motion branch chains will move and rotate to either compress or stretch the connected spring in order to compensate for the position and orientation.

A sectional view of the motion branch chain along the front and rear sliding rod axial directions is shown in Fig. 3. The sleeve is fixed on the moving platform, and the front and rear sliding rods connect to the sleeve by the column pair. The front and rear sliding rods can move forward and backward relative to the sleeve and can also rotate to a small angle around their own axes. The front and rear sliding rods are fixed together using a C-type component, and the connections between the C-type component and up and down sliding rods, and front and rear sliding rods are all column pairs. Therefore, each motion branch chain works on the principle of parallel mechanism of the CCC type. Considering the assembly

factors, the up and down sliding rods are made of three components, and the left and right sliding rods pass through a hole in the middle section.

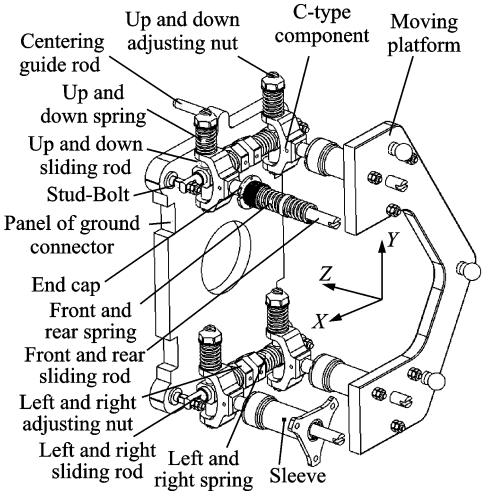

Fig. 2 Illustration of position and orientation compensation mechanism

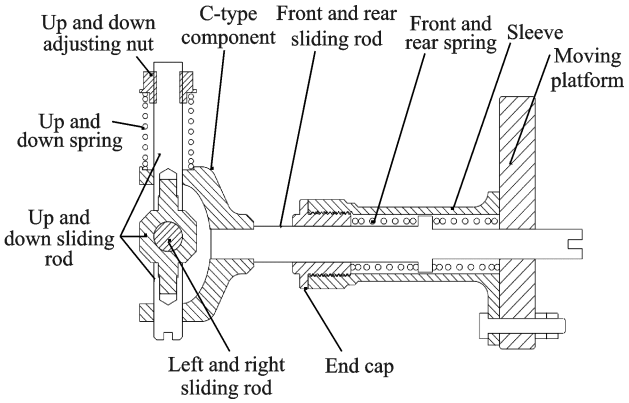

Fig. 3 Sectional view of a moving branch along axial direction of the front and rear sliding rods

The local view of the left and right sliding rods is shown in Fig. 4. The left and right sliding rods are secured to the ground connector panelusing a studbolt. One end of the left and right springs acts on the up and down sliding rods, and their other end acts on the left and right adjusting nuts. The ground connector panel shifts left and right and can be controlled by compressing and stretching the left and right springs. The up and down springs fully support the weight on the ground connector panel, and the weight is transferred directly to the up and down sliding rods through the left and right sliding rods. When the front and rear positions of the ground connector

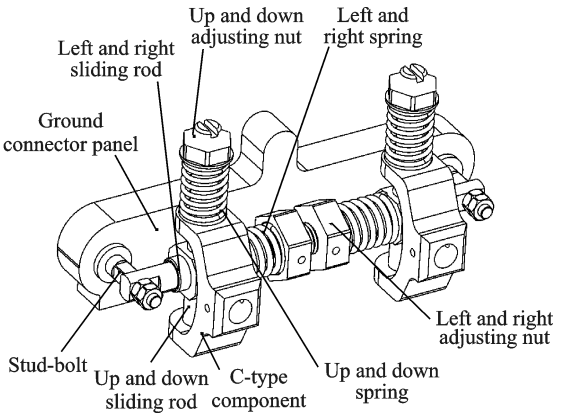

Fig. 4 Illustration of the left and right sliding rods

panel change relative to the moving platform, only the front and rear springs are deformed while the others are not.

According to the installation position of a spring, the springs within the four motion branch chains can be divided into three groups: (1) front and rear, (2) up and down, and (3) left and right. The first, second, and third groups contain eight, four, and four chains, respectively. There are more springs in the front and rear spring groups, and the global stiffness is greater to provide a sufficient docking force. The up and down spring group carries most of the weight of the ground connector panel, with possible mass eccentricity, and the position and orientation are adjusted according to the amount of compressionpresent in the up and down springs. Due to the specificity of the relative position of the four motion branch chain structures, the degrees of freedom of the ground connector panel relative to the moving platform are decoupled in the three translational directions. Therefore, more space is required for the compensation mechanism, and adjustments are more convenient. The structure has a certain amount of stability and anti-interference ability. Moreover, the compensation mechanism can be restored to the initial position with re-docking capabilities after docking and filling have been completed, and the ground connector panel and rocket connector panel are disengaged.

1.4 Design of spring stiffness

The docking process can be divided into two

stages: The reaching servo stage before docking and the servo stage after docking, which have opposite stiffness requirements for the position and orientation compensation mechanism. The reaching servo stage requires the stiffness to be as high as possible since the effect of inertial forces will be smaller in this case. Excessive shaking of the ground connector panel relative to the moving platform will not occur, improving the docking accuracy. The servo stage requires the stiffness of the position and orientation mechanism to be as low as possible resulting in smaller forces acting on the rocket panel. The spring stiffness is the main factor affecting the overall stiffness of the compensation mechanism. Therefore, the spring stiffness should be reduced as much as possible to minimize shaking below threshold level. To validate the relevant technical indexes required by the mechanism to meet the docking requirements, three sets of design parameter variables for the spring stiffness were determined, and an objective function of the *XYZ* deviation was established. The effect of each design parameter on the objective function was analyzed by the optimal calculation method in ADAMS, and the spring stiffness was optimized under the actual working conditions. According to the optimization results, the stiffness of the up and down springs, left and right springs, and front and rear springs was determined to be 11, 26, and 20 N/mm, respectively.

2 Simulation of Docking Process Under the Maximum Deviation

During the reaching servo stage, greater docking deviation results in greater contact forces on the rocket. Therefore, analyzing the maximum contact impact force on the rocket under the maximum docking deviation is of importance.

2.1 Establishment of the dynamic model

A dynamic model of the position and orientation compensation mechanism was established in ADAMS. The origin of the kinematic model was set as the origin of the coordinate system shown in Fig. 2. After assigning the component quality attributes, the coordinate system of each component in the model was automatically generated, with the origin corresponding to the centroid of the component. The quality attribute of the imported model was then matched, and constraint processing was carried out according to the connection relationship between the components. A fixed secondary connection was used between the moving platform and sleeve and between the left and right sliding rods and ground connector panel. A column pair connection was used between the front and rear sliding rods and sleeve, the up and down sliding rods and front and rear sliding rods, and the left and right sliding rods and up and down sliding rods. In each motion branch chain, the spring was set on the sliding rod. The dynamic model of the compensation mechanism is shown in Fig. 5.

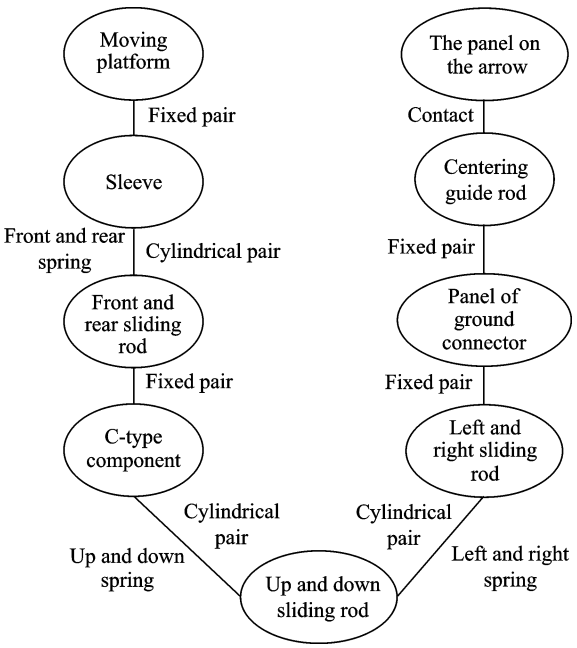

Fig. 5 Topological structure of the dynamic model

2.2 Simulation of docking process under the maximum deviation

To simulate the docking process under maximum deviation, a constant deviation of $\Delta L_x = 8$ mm and $\Delta L_y = 8$ mm of the center position of the moving platform relative to the center position of the rocket connector panel was set in advance in the *X*- and *Y*-directions, respectively,

and no deviation in the Z-direction. In the time range 0—6.2 s, the ground connector panel approaches the rocket connector panel. At 6.2 s, the centering guide rod on the ground connector panel comes into contact with the taper hole on the panel of the rocket connector, beginning the docking process. In the X-direction, the variation in the collision force exerted by the centering guide rod and resulting force F over time is shown in Fig. 6. In the Y- and Z-directions, the variation in the force exerted on the rocket and resulting force over time is shown in Figs. 7, 8, respectively.

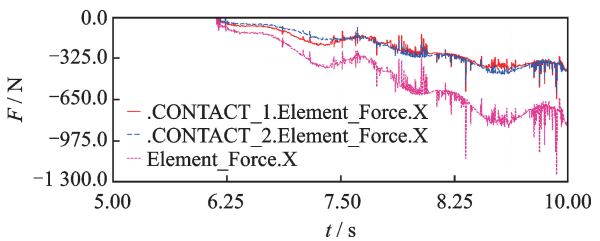

Fig. 6 Variation in the collision force exerted by centering guide rod and resulting force in the X-direction over time

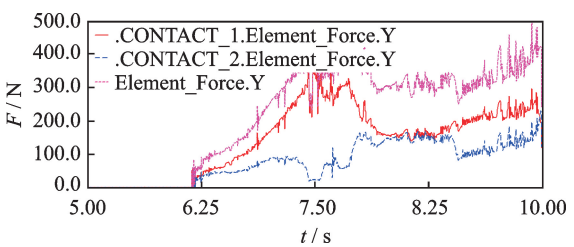

Fig. 7 Variation in the collision force exerted by centering guide rod and resulting force in the Y-direction over time

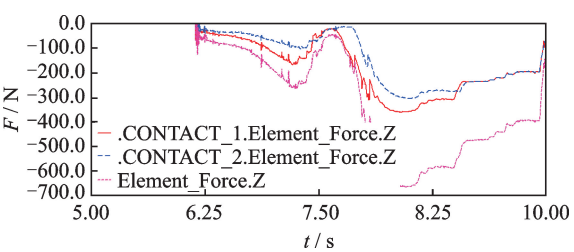

Fig. 8 Variation in the collision force exerted by centering guide rod and resulting force in the Z-direction over time

Figs. 6, 7 show that the contact forces in both the X- and Y-directions in crease as the centering guide rod penetrates deeper into the tapered hole. The force on the rocket reaches a value of 823 N in the X-direction and 426 N in the Y-direction for a deviation of 8 mm. The peak forces reached 1 235 N and 496 N, in the X- and Y-directions, respectively, due to the contact collision. As shown in Fig. 8, as the contact penetrates deeper, the contact force in Z-direction changes from small to large and then small again. After docking, the contact force in the Z-direction is 50 N, and the maximum contact force during the process is 665 N.

In summary, under the maximum docking deviation, the contact force of the rocket in the X, Y, and Z-directions satisfies the requirement of a contact collision force no greater than 3 000 N.

3 Test of Position and Orientation Compensation Mechanism Prototype

3.1 Test summary

The performance of the automatic docking device was verified by the bench testing, as shown in Fig. 9. According to the structural characteristics of the position and orientation compensation mechanism, the maximum force of the rocketina single translational direction is mainly derived from the force when the compensation mechanism reaches the maximum compensation value. The test was carried out to verify whether the compensation space in each direction of the compensation mechanism meets the requirements and ensure the external force acting on the rocket remains within an appropriate range.

The theoretical stiffness values of the up and

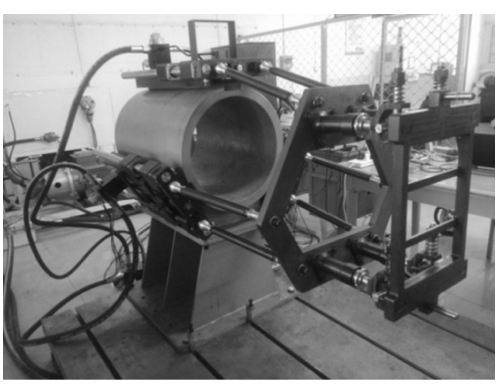

Fig. 9 Illustration of bench testing equipment for automatic docking device

down springs, left and right springs, and front and rear springs are 11, 26, and 20 N/mm, respectively. The actual stiffness values are 10.51, 25.53, and 19.92, respectively. Therefore, the error is within ±1 N/mm.

The ground connector panel was set to the vertical state and the up and down adjusting nuts, left and right adjusting nuts, and end cap were adjusted to create a symmetrical structure. At this time, the position and orientation compensation mechanism was in the initial working state, and the translational and rotational effects were examined by applying the load in three translational and three rotational directions. After verifying that the compensation mechanism meets the space requirements for six degrees of freedom, the maximum load test and maximum deviation test were carried out. Before taking the measurements, the hydraulic cylinder was retracted to its limit to ensure constant position of the moving platform.

3.2 Maximum load test

When the position and orientation compensation mechanism was in the initial working condition, a mass of 50 kg was applied to the ground-connector panel so that the up and down springs were compressed with an 8 mm workload. The weight was then removed after a certain period of time, and the compensation mechanism was restored to its original condition. During this process, the working states of all parts of the compensation mechanism were normal, and no parts were damaged.

3.3 Maximum deviation test

An S tension-compression sensor with a sensitivity of 2.0 mV/V and maximum range of 300 kg was used to measure the force during the maximum deviation test. As shown in Fig. 10, a sensor is placed between the ground connector panel and rocket connector panel. The rocket simulator was used to move the rocket connector panel by 8 mm to the front and rear (Z-direction), up and down (Y-direction), and left and right (X-direction), respectively, and the moving values were read froma scale on therocket simulator, as shown in Fig. 11. After the output value of the S tension-compression sensor was measured, the force was calculated using the formula $F=k\times L$, where k is the stiffness of the S type pull pressure sensor, and L is the displacement value.

Since the same force acts on the same length during tension and compression, measurements were only taken under compression.

Fig. 10 Position of sensor on the rocket simulator

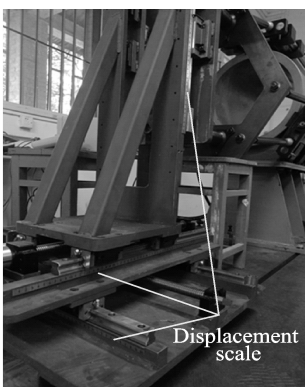

Fig. 11 Position of displacement scale on the rocket simulator

For each of the three spring groups, the ground connector panel was moved 8 mm, and the theoretical values of the resultant forces were calculated.

For a deviation of 8 mm between the ground connector panel and rocket connector panel in the front and rear, left and right, and up and down directions, the measured values are listed in Table 1. The actual force values were obtained by substituting the measured values into the formula. The voltage values measured using the S tension-compression sensor, calculated force values,

theoretical spring force values, and simulation contact force values under the maximum docking deviation are listed in Table 1.

Table 1 Voltage values, tested force values, theoretical values of spring force and simulation contact force values

Project	Left and right (X)	Up and down (Y)	Front and rear (Z)
Voltage value/mV	11.0	4.4	17.4
Tested force value/N	808.5	323.4	1 278.9
Theoretical value of the spring force/N	816.9	336.3	1 274.9
Simulation contact force value/N	823.2	353.8	

For a deviation of 8 mm, the three force values were relatively constant in the X- and Y-directions, including the tested force value, theoretical spring force value, and contact force value, as listed in Table 1. In the Z-direction, only the tested force value was consistent with the theoretical spring force value of spring.

Fig. 12 is a sketch map of the four vertices at the bottom of the rocket simulator. By adding gaskets at points 2 and 3, the rocket simulator produces a rotation of 0.5°. During this process, the working states of all the parts based on the compensation mechanism were normal and no parts were damaged.

Fig. 12 Sketch map of four vertices at the bottom of rocket simulator

4 Conclusions

In this study, the rigid connection between the connector docking device and arrow body was transformed into a flexible connection by a position and orientation compensation mechanism. The position and orientation compensation mechanism was designed to have a simple structure and large load bearing capacity, occupy a small volume, and offer simple installation and adjustment. It effectively reduced the ripping force of the arrows and improved the adaptability of the automatic docking process to the environment. Based on the bench testing of the automatic docking device and the simulation of the docking process under the maximum docking deviation, the following conclusions were made:

(1) The position and orientation compensation mechanism meets the requirements including a maximum compensation of ±8 mm in the three translational directions and ±0.5° in the three rotational directions.

(2) According to the maximum deviation test, the requirement for the compensation mechanism to support a mass of 50 kg was met.

(3) A simulation of the docking process proved that for a maximum single direction displacement, the pressure value of the arrow is within the allowable range of no more than 3 000 N. The simulation results were verified by the maximum deviation test. In the X- and Y-directions, the experimental force value and simulation contact force were consistent with the theoretical spring force value. The test force value in the Z-direction was also consistent with the spring force theory. These results demonstrate that the spring stiffness is the most important factor in determining the overall stiffness of the position and orientation compensation mechanism.

References:

[1] WANG Lixing. Analysis of automatic docking technology for Russian rockets[J]. Aerospace Launch Technology, 2003 (1): 45-50. (in Chinese)

[2] GOSSELIN A M. Automated ground umbilical systems project [C]//Space Visions Congress. Cocoa Beach, FL, USA: NASA, 2007:20130011368.

[3] HOUSHANGI N. Autonomous robotic positioning umbilical system[C]//2000 IEEE International Conference on Systems, Man and Cybernetics. Nashville, TN, USA: IEEE, 2000,4:2981-2986.

[4] RUDOLPH A. Operational experience with the Saturn V[J]. Nuclear Science IEEE Transactions on, 2013, 49 (3):1071-1076.

[5] Jr TATEM B C. Rolling beam umbilical system[J]. NASA Kennedy Space Center, 1981: 289-303.

[6] JUNG I H, HWANG D K. Control of mechanical ground support equipment for Korean launch complex [C]//AIAC14 Fourteenth Australian International Aerospace Congress. Australia: [s. n.], 2011: 242-249.

[7] WEN Jing, DUN Xiangming, ZHANG Yulin. Research on present situation and development trend of automatic filling and disengagement robot for propellant filling[J]. Robot Technology and Application, 2010(6): 20-22. (in Chinese)

[8] HUANG Chao. Implementation of automatic butt connector, design and study of suspension system [D]. Nanjing: Nanjing University of Science and Technology, 2015: 1-57. (in Chinese)

[9] XIANG Ming, SHEN Tingzheng, ZHONG Renquan. Rocket variable stiffness multi axis docking mechanism. China, 101398278[P]. 2009-04-01. (in Chinese)

[10] ZHAO Shuaifeng. Design and experiment of a control system for automatic docking of propellant and automatic arrows module of exfoliative robot[J]. Robot, 2012(3): 307-313. (in Chinese)

[11] HUANG Xiaoni, XIANG Ming, ZHANG Yulin. The design of the automatic docking of propellant and the body of the exfoliative robot[J]. Robot, 2010, 32 (2): 145-149. (in Chinese)

[12] DOUG G, FRED J, MARK M C. Hydrogen vent ground umbilical quick disconnect flight seal advanced development [J]. Engineering Services Contract, 2009: KSC-2012-127.

[13] HAN Xianguo, CHEN Wuyi. Analysis of kinematic characteristics of 3-PSS parallel mechanism based on screw theory [J]. Machine Tool and Hydraulic, 2005 (12): 22-24. (in Chinese)

[14] Van DORSSER W D, BARENTS R. Gravity-balanced arm support with energy-free adjustment[J]. Journal of Medical Devices, 2007(1): 151-156.

[15] DUAN Qihan. Dynamics analysis of 3-PRRU parallel robot [D]. Hangzhou: Zhejiang Sci-Tech University, 2011: 17-20. (in Chinese)

[16] MEI Lai. Parallel robot[M]. Beijing: Mechanical Industry Press, 2012: 58-60. (in Chinese)

[17] ZHENG Guokun, WANG Xiaojun, LI Daoping. Research on control process of automatic docking system based on launch vehicle discharge connector[J]. Missile and Space Transport Technology, 2015 (1): 25-28. (in Chinese)

[18] SHI Haoming. Dynamic analysis and optimization design of 6-PUS parallel mechanism[D]. Chongqing: Chongqing University, 2012: 2-11. (in Chinese)

Mr. **Zhou Cheng** received the marster's degree in mechanical design and theory from Nanjing University of Science and Technology in 2011 and then joined in Nanjing University of Science and Technology. Now he is a Ph. D. student in mechanical engineering at Nanjing University of Science and Technology. His research is focused on digital design.

Mr. **Yu Cungui** received his Ph. D. degree in weapon science and technology from Nanjing University of Science and Technology in 2011 and joined in Nanjing University of Science and Technology. His research is focused on weapon launching theory and technology.

(Production Editor: Zhang Huangqun)